

# A Robust UAV-UGV Collaborative Framework for Persistent Surveillance in Disaster Management Applications

Md Safwan Mondal<sup>1,†</sup>, Subramanian Ramasamy<sup>1</sup>, James D. Humann<sup>2</sup>, James M. Dotterweich<sup>3</sup>, Jean-Paul F. Reddinger<sup>3</sup>, Marshal A. Childers<sup>3</sup>, Pranav Bhounsule<sup>1</sup>

**Abstract**— Unmanned Aerial Vehicles (UAVs) are fast, agile, and capable of covering large areas quickly but are constrained by their limited fuel capacities. In contrast, Unmanned Ground Vehicles (UGVs) have longer battery lives but move at slower speeds. By combining UAVs with UGVs, which serve as mobile recharging stations, we can harness the strengths of both: UAVs can achieve rapid task execution over extended periods by refueling from UGVs. This synergy makes the collaborative routing of UAVs and UGVs well-suited for modern disaster management applications. However, their varied operational constraints require a sophisticated planning framework to ensure optimized coordination and task execution. In this paper, we introduce a robust multi-agent framework leveraging asynchronous planning to optimize the routes of UAVs and UGVs in a persistent surveillance task, considering their individual limitations like fuel, speed, and charging constraints. The framework is designed to scale effectively with the number of vehicles and accommodates diverse team configurations. The effectiveness of this framework is demonstrated through a simulation of a 4-hour mission covering 30 task points across five different team compositions, showing significant improvements in route efficiency. Additionally, a detailed cost analysis identifies the optimal UAV-UGV team composition by effectively balancing mission performance and cost, thus serving as a valuable tool for optimizing disaster response strategies.

## I. INTRODUCTION

The rapid advancement of Unmanned Aerial Vehicles (UAVs) has significantly expanded their applications in modern disaster management systems [1]–[3]. UAVs, notable for their speed, cost-effectiveness, and ability to navigate challenging terrains, have proven their versatility in varied scenarios. For instance, in Yuyao, China [4], UAVs were employed to capture optical imagery for monitoring urban water-logging during flood mapping. Similarly, in Tehran [5], UAVs facilitated emergency commodity transportation for post-earthquake resource distribution, and during the La Conchita mudslide [6], UAVs contributed to conducting rescue operations. Despite their capabilities, a major limitation of UAVs is their restricted battery capacity, which hinders

<sup>1</sup>Md Safwan Mondal, Subramanian Ramasamy and Pranav A. Bhounsule are with the Department of Mechanical and Industrial Engineering, University of Illinois Chicago, IL, 60607 USA. mmonda4@uic.edu, sramas21@uic.edu, pranav@uic.edu <sup>2</sup>James D. Humann is with DEVCOM Army Research Laboratory, Los Angeles, CA, 90094 USA. james.d.humann.civ@army.mil <sup>3</sup>James M. Dotterweich, Jean-Paul F. Reddinger, Marshal A. Childers are with DEVCOM Army Research Laboratory, Aberdeen Proving Grounds, Aberdeen, MD 21005 USA. james.m.dotterweich.civ@army.mil, jean-paul.f.reddinger.civ@army.mil, marshal.a.childers.civ@army.mil

† Corresponding author, \*This work was supported by ARO grant W911NF-14-S-003.

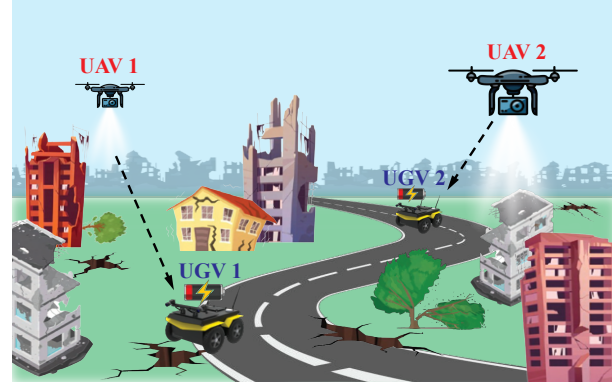


**Fig. 1:** Illustration of collaboration between UAVs and UGVs in surveying disaster-stricken zones. UAVs conduct continuous surveillance of impacted areas and recharge via UGVs.

continuous operation during extended missions. To overcome this, UAVs can be periodically recharged, either from fixed depots or mobile charging stations. However, fixed refueling stops, due to their stationary nature, can constrain the operational range of UAVs. Hence, Unmanned Ground Vehicles (UGVs) are utilized as mobile recharging bases that provide ground support to UAVs and conduct surveillance along the roads, ensuring comprehensive and continuous coverage in disaster management operations [7]. Thus the collaboration between UAVs and UGVs becomes essential in both pre- and post-disaster management applications.

This article examines a multi-agent collaborative system between UAVs and UGVs, designed for conducting surveillance in regions impacted by disasters, enabling continuous monitoring and reconnaissance. To mirror the complexities of real-world situations, we have imposed constraints on the vehicles. The UAVs operate under limited battery endurance and can only get recharged from the UGVs that are restricted to travel on the road network only in limited speed bound. The UGVs also have capacity constraints as they can only support one UAV at a time during the recharging process. This heterogeneity in the vehicle characteristics thus underscores the need for strategic planning of UAV and UGV routes, as well as their coordination for recharging, to ensure consistent coverage of disaster-affected sites.

## A. Related studies

Over the years, comprehensive research has been conducted on the use of aerial mobility in disaster management [1]–[3]. Maza et al. [8] developed a distributed decision-making architecture for task allocations in multi-UAV sys-

tems to perform a variety of missions, such as surveillance, sensor deployment, and fire threat detection, demonstrating its practical applicability. Erdelj et al. [9] conducted a comprehensive survey on the utilization of UAVs in disaster management. Their work explored how UAVs are used for surveying disaster-affected areas, establishing wireless communication links, and understanding the interaction between different disaster classes and UAVs equipped with wireless sensors. Similarly, Nikhil et al. [10] focused on the importance of communication technologies in UAV-based disaster management systems. Their research covered critical areas such as early warning systems, emergency communication, and image processing techniques. Scherer et al. [11] considered the energy and communication constraints of the UAVs in surveillance tasks, introduced an offline path planning algorithm for multiple UAVs, and analyzed how base station configurations affect mission performance. Hayat et al. [12] introduced a multi-objective optimization algorithm for task allocation and path planning within UAV teams, achieving a significant reduction in overall mission completion times by up to 65% in search and rescue scenarios.

UAV-UGV cooperative routing problems are often modeled as optimization problems with previous attempts of solving them as two-echelon routing problems. Gao et al. [13] showed the approach of commanding cooperative UGV and UAV for emergency resource delivery by modeling it as a nested vehicle routing problem. They presented mixed integer programming formulation and an iterative improvement algorithm that can solve the problem 10% faster. Ramasamy et al. [14] explored the potential of hyperparameter tuning with Bayesian Optimization and Genetic Algorithms to enhance the solution quality of UAV-UGV cooperative routing. Their work was further expanded through a more generalized approach using the A-Teams architecture, significantly boosting computational efficiency in solving the problem [15]. UAV-UGV cooperative routing problem has also been experimentally validated in lab-scale setups. Leahy et al. [16] developed automata-based techniques for generating collision-free motion plans for vehicle teams, ensuring compliance with temporal logic constraints. In our previous study [17], we also validated a bilevel optimization algorithm using a single UAV-UGV team in a laboratory setting. Cooperative routing problems are also extended to multi-UAV-UGV team settings; Chour et al. [18] tackled a UAV-UGV rendezvous challenge for sustained operations with their proposed multi-level coordination, scheduling, and planning algorithm. In a related problem, authors of [19], [20] proposed a scalable and robust approximation algorithm for persistent surveillance by energy-constrained UAVs and UGVs, relying on forming uniform UAV-UGV teams and partitioning the environment among them. However, these methodologies often overlook practical constraints, such as UGV capacity and speed limitations, and fail to scale with an increasing number of vehicles, which are crucial in disaster scenarios.

In this study, we introduce a robust planning framework designed to accommodate various UAV-UGV team compo-

sitions and effectively scale with the number of vehicles, while addressing the practical constraints of these vehicles. Employing a tiered, iterative approach, our framework meticulously designs the UAV-UGV routes and schedules their recharging times, ensuring optimal persistent surveillance of disaster sites. The framework's effectiveness is demonstrated through simulations conducted on a real-world disaster site as a case study. The main contributions of our study are as follows:

- 1) Modeling a new constrained multi UAV-UGV routing problem for disaster scenarios, incorporating UAV fuel limits and UGV speed and capacity constraints, making it highly applicable to disaster management applications.
- 2) Developing of a robust, iterative planning framework for multi-agent systems that enables collaborative routing across diverse team compositions. The framework efficiently scales with more vehicles due to its asynchronous planning architecture.
- 3) Implementing our framework in a real-world case study with varied UAV-UGV teams, showcasing the approach's effectiveness and real-world viability.

## II. PROBLEM STATEMENT

As a demonstrative application of UAV-UGV collaborative routing for disaster management, we focus on a ‘persistent surveillance problem’ at a disaster site. Persistent surveillance involves continuous monitoring of an area or site for an extended period to collect real-time information. It plays a crucial role in both pre- and post-disaster scenarios, assisting in tasks such as damage assessment, search and rescue operations, delivery of emergency relief supplies, and other critical functions. To define the problem formally, let us consider a system consisting of a set of UAVs  $\mathcal{A} = \{u_j^a, \forall j = 1, \dots, M\}$  and UGVs  $\mathcal{G} = \{u_i^g, \forall i = 1, \dots, N\}$  that will be continuously visiting a set of target nodes  $\mathcal{M} = \{m_k, \forall k = 1, \dots, n\}$  across a disaster scenario. The task nodes needed to be routinely visited by either a UAV or UGV, with the *age period* metric  $a^k = t - t_{last}^k$  determining the time elapsed since the last visit to the node  $m_k$ . For reinforcing persistent visits to the task nodes so that the most recent data are always collected from the disaster sites, we define *score metric* as:

$$S = \frac{1}{\alpha} \sum_{k=1}^n \sum_{q=1}^p (t_q^k - t_{q-1}^k)^3 = \frac{1}{\alpha} \sum_{k=1}^n \sum_{q=1}^p (a_q^k)^3 \quad (1)$$

Here,  $t_0^k, t_1^k, \dots, t_p^k$  are the time instances in the ascending order when a task node  $m_k$  is visited during the mission period. Here,  $\alpha$  is a constant number used to scale down the *score metric* value; we choose  $\alpha = 27 \times 10^5$ . The *score metric* is designed to be cubic in time to penalize the longer inter-visit harshly. The objective is to strategize a collaborative operation between the UAVs and UGVs to keep the *score metric* value as low as possible at the end of the entire task.

The UAVs and UGVs share heterogeneous traits (based on the model in [21]) as the UAVs have a limited fuel capacity

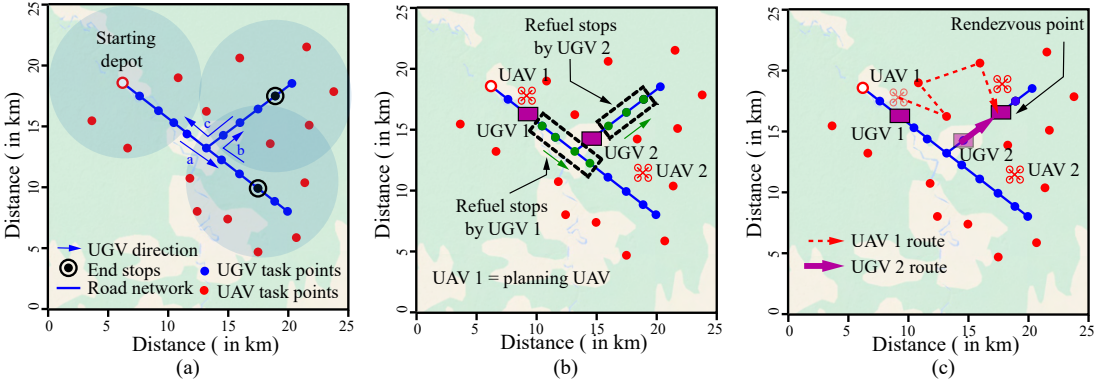


**Fig. 2:** *UGVPlanner* Working Principles. a) First, end stops and UGVs' traversal directions are derived by solving the Minimum Set Cover problem; here blue circles represent the radial coverage of UAVs b) Second, available refuel stops from two UGVs when planning for UAV1 in a 2 UAVs-2 UGVs system c) Third, UGV2 and UAV1 routes and rendezvous between them

$F^a$  and can fly faster with their power consumption model  $\mathcal{P}^a = 0.0461(v^a)^3 - 0.5834(v^a)^2 - 1.8761v^a + 229.6$ , a function of their flying velocity  $v^a$ . Contrastingly, the UGVs are restricted to traveling on the road network with limited speed  $v^g$  and can refuel the UAVs by acting as a mobile recharging station. The UGVs follow the power consumption model  $\mathcal{P}^g = 464.8v^g + 356.3$  and for simplification, we have not considered fuel constraints on the UGVs.

The recharging process of the UAVs on the UGVs is not instantaneous as the recharging time  $t_{Re}^a$  depends on the UAV's fuel consumption  $E^a$  in flight. It can be determined as :

$$t_{Re}^a = \frac{E^a}{\beta} = \frac{\mathcal{P}^a \times (t_e^a - t_s^a)}{\beta} \quad (2)$$

Here,  $t_s^a$  and  $t_e^a$  are the UAV's flight starting and end times and  $\beta = 310.8$  (from [21]). We also consider the capacity constraint of the UGVs so that one UGV can recharge one UAV at a time, which increases the complexity of the problem, as it adds the aspect of conflict-free scheduling in the planning framework.

Hence, we present a multi-level framework that demonstrates robustness in managing different configurations of UAV-UGV teams, optimizing routes for both UGVs and UAVs through its multiple planning levels. Within the framework, the *UAVPlanner* and *UGVPlanner* efficiently optimize route sorties for UAVs and UGVs respectively. Additionally, the *RechargePlanner* schedules conflict-free recharging instances between them to ensure persistent coverage over the task nodes during the prolonged operation.

### III. METHODOLOGY

In the optimization framework, the three major levels *UGVPlanner*, *UAVPlanner* and *RechargePlanner* interact with each other to plan the routes for the UAVs and UGVs asynchronously. The asynchronous planning approach considers one vehicle at a time, taking into account the conditions posed by the other vehicles. It also adds the advantages of scalability as you can extend the number of UAVs and UGVs in the scenario. We have discussed each individual block in detail:

#### A. UGV Planner

The *UGVPlanner* plays a pivotal role in the planning framework, executing three distinct operations at different stages.

##### 1) UGV direction setting

The initial operation '*UGV direction setting*' occurs as a one-time process at the inception of the planning cycle. During this phase, the *UGVPlanner* determines the operational range of the UGVs within the road network by solving a Minimum Set Cover (MSC) problem [22]. In this context, task nodes  $\mathcal{M}$  serve as target locations, while the fuel capacity of UAVs  $F^a$  defines the coverage radius. The MSC problem aids in identifying the essential end stops  $\mathcal{R}_e$  to ensure that all the task nodes are accessible to the UAVs from the road network. Once these end stops  $\mathcal{R}_e$  are identified, the algorithm proceeds to optimize UGV routes by solving a Traveling Salesman Problem (TSP) with the end stops. This TSP calculation determines the most efficient traversal direction  $\bar{X}_{g,i}$  of the UGVs from their respective initial positions, i.e.,  $x_0^{g,i}, \forall u_i^g \in \mathcal{G}$ . The solution to a sample scenario is visually represented in figure 2a, illustrating the end stops and the UGVs' traversal directions as derived from MSC. Application of Minimum Set Cover problem for obtaining the UGV traversal direction has been previously explored by Maini et al. [23] and further details can be found in our previous works [17], [24].

##### 2) Rendezvous scheduling

The '*Rendezvous scheduling*' operation is executed by the *UGVPlanner* each time the *UAVPlanner* plans for a UAV  $u_{j=p}^a$ . To facilitate this process, the *UGVPlanner* maintains a dictionary *UGVinstances* that has structured lists for all the UGVs containing tuples that represent UGVs' coordinate positions at various time points in the global time frame, as defined below:

$$\text{UGVinstances} = \{[(x^{g,i}, t^{g,i}) \text{ at } t^{g,i} \in {}^G\mathbf{T}^{g,i}], \forall u_i^g \in \mathcal{G}\}$$

here,  ${}^G\mathbf{T}^{g,i} = [{}^Gt_0^{g,i}, {}^Gt_1^{g,i}, \dots, {}^Gt_n^{g,i}]$  represents the global time dimension for UGV  $u_i^g$ .

Then utilizing the *UGVinstances*, we determine the locations and times from where and when the UGVs will be available to support the planning UAV  $u_{j=p}^a$  for recharging.

In the time dimension  ${}^G\mathbf{T}^{g,i}$  of each UGV, the UGV  $u_i^g$  will be available only after its last time step  $t = {}^Gt_n^{g,i}$ , because choosing any time step prior to last time step would intervene the already planned routes and also the UGV has a capacity constraint that it can support only one UAV at a time. Hence, UGVs can only become available after their last timesteps in time dimension in the  $UGVinstances$  for conflict-free scheduling of UAVs.

For each UGV the availability time is  ${}^Gt_s^{g,i} = {}^Gt_n^{g,i}$  and the position at that time is its availability position  $x_s^{g,i}$ . We can utilize the availability position  $x_s^{g,i}$  and moving direction  $\vec{\mathbf{X}}^{g,i}$  to determine the potential refuel stops offered by a UGV. The locations on the road network along  $\vec{\mathbf{X}}^{g,i}$  that a UGV  $u_i^g$  with speed  $v^g$  can reach within the maximum flight duration time ( $T_f = \frac{F^a}{P^a}$ ) of a UAV are considered as potential refueling stops provided by that UGV. The refuel stops  $X^r$  from all UGVs can be calculated as :

$$X^r = [ \{x^{g,i} \mid \frac{\|x^{g,i} - x_s^{g,i}\|}{v^g} \leq T_f\}, \forall u_i^g \in \mathcal{G} ] \quad (3)$$

Once, the potential refuel stops offered by a UGV are identified (see figure 2b), the time windows for them are calculated. First, we calculate the lower limits of the time windows in the global time frame, denoting them as  ${}^Glr^i$  :

$${}^Glr^i = {}^Gt_s^{g,i} + \frac{\|x^{g,i} - x_s^{g,i}\|}{v^g}, \forall x^{g,i} \in X^r \quad (4)$$

If the planning instance time of the planning UAV  $u_{j=p}^a$  in the global time frame is  ${}^Gt_s^{a,j=p}$ , we can transfer  ${}^Glr^i$  to the local time frame of that UAV, denoting it as  ${}^Llr^i$  :

$${}^Llr^i = {}^Glr^i - {}^Gt_s^{a,j=p}, \forall x^{g,i} \in X^r \quad (5)$$

If any UGV has  ${}^Gt_s^{g,i} \geq {}^Gt_s^{a,j=p}$ , it limits the UAV's allowable return time  ${}^Gt_e^{a,j=p}$  on any of its offered refuel stops. This limitation is due to the potential need for that UGV to assist other UAVs in future timesteps. Quantitatively, the sum of the UAV's return time  ${}^Gt_e^{a,j=p}$  and its recharging duration  $t_{Re}^{a,j=p} = \frac{P^a}{\beta}({}^Gt_e^{a,j=p} - {}^Gt_s^{a,j=p})$  (derived using Eq. 2), must be within the UAV's maximum flight time  $T_f$ , when subtracted from that UGV's availability time  ${}^Gt_s^{g,i}$ . The maximum allowable return time in the global time frame, (denoted as  ${}^Gt_e^{a,j=p}$ ) for the UAV  $u_{j=p}^a$  at any refuel stop of UGV  $u_i^g$  is calculated as:

$$\begin{aligned} & {}^Gt_e^{a,j=p} + t_{Re}^{a,j=p} - {}^Gt_s^{g,i} \leq T_f \\ \Rightarrow & (1 + \frac{P^a}{\beta}) {}^Gt_e^{a,j=p} - \frac{P^a}{\beta} {}^Gt_s^{a,j=p} \leq T_f + {}^Gt_s^{g,i} \end{aligned} \quad (6)$$

Since, in the UAV's local time frame,  ${}^Lt_e^{a,j=p} = {}^Gt_e^{a,j=p} - {}^Gt_s^{a,j=p}$ , the UAV's allowable flight end time in local time frame, ( denoted as  ${}^Ll_e^{a,j}$ ) can be calculated as follows:

$$\begin{aligned} & (1 + \frac{P^a}{\beta}) {}^Ll_e^{a,j} \leq T_f + ({}^Gt_s^{g,i} - {}^Gt_s^{a,j=p}) \\ \Rightarrow & {}^Ll_e^{a,j} \leq \frac{\beta}{\beta + P^a} (T_f + ({}^Gt_s^{g,i} - {}^Gt_s^{a,j=p})) \end{aligned} \quad (7)$$

These maximum allowable return times ( ${}^Ll_e^{a,j}$ ) serve as the higher limits ( ${}^Lh^{r,i}$ ) of refuel stops' time windows on

---

### Algorithm 1: UGV Planner Algorithm

---

```

Input: Task nodes  $\mathcal{M}$ , UAV fuel capacity  $F^a$ ,  $UGVinstances$ ,  $UAVPlanner$ 
Output: Updated  $UGVinstances$ 

1 Initialize End Stops:  $\mathcal{R}_e \leftarrow MSC(\mathcal{M}, F^a)$ 
2 if Planning time == 0 then
3   Perform initial UGV direction setting
4   foreach  $u_i^g$  in  $\mathcal{G}$  do
5     Set starting position  $x_0^{g,i}$ 
6     Determine traversal direction  $\vec{\mathbf{X}}^{g,i} \leftarrow TSP(x_0^{g,i} + \mathcal{R}_e)$ 
7 if  $UAVPlanner(u_{j=p}^a)$  is Active then
8   Perform Rendezvous scheduling
9   foreach  $u_i^g$  in  $\mathcal{G}$  do
10    Calculate refuel stops with time windows  $\{X^r, T^r\}$  along  $\vec{\mathbf{X}}^{g,i}$ 
11    Send  $\{X^r, T^r\} \rightarrow UAVPlanner(u_{j=p}^a)$ 
12    Get rendezvous details  $x^R, t^R, u_{i=R}^g \leftarrow UAVPlanner(u_{j=p}^a)$ 
13   Perform UGV sortie formation
14   for  $u_{i=R}^g$  in  $\mathcal{G}$  do
15     Create route sortie  $\tau_{i=R}^g$ 
16     Update  $UGVinstances[u_{i=R}^g]$ 
17 return  $UGVinstances$ 

```

---

respective refuel stops; i.e.,  ${}^Lh^{r,i} = {}^Ll_e^{a,j=p}$ ,  $\forall x^{g,i} \in X^r$ . Together the lower and higher limits constitute the refuel stops' time windows,  $T^r = \{({}^Ll_e^{r,i}, {}^Lh^{r,i})\}$ ,  $\forall x^{g,i} \in X^r$ . The  $UGVPlanner$  then communicates these refuel stops' information  $\{X^r, T^r\}$  with  $UAVPlanner$  to formulate a route plan for the UAV  $u_{j=p}^a$  and determine the rendezvous location  $x^R$ , time  $t^R$ , and the UGV  $u_{i=R}^g$  which will recharge the UAV  $u_{j=p}^a$ .

#### 3) UGV sortie formation

The final operation within the  $UGVPlanner$  is 'UGV sortie formation'. During this phase, using the rendezvous information obtained in the previous step, the  $UGVPlanner$  connects the recharging UGV's  $u_{i=R}^g$  availability position  $x_s^{g,i=R}$  to the designated rendezvous point  $x^R$  and we get the spatial information  $x^{g,i=R}$  of its sortie. We also get the temporal elements  $t^{g,i=R}$  using UGV's speed by calculating UGV's arrival time at those coordinates. In a case when a UGV reaches a refueling stop before the UAV, it is programmed to wait, ensuring synchronized coordination between them. Consequently, the  $UGVPlanner$  provides a complete view of the route sortie  $\tau_{i=R}^g$ , encompassing both spatial and temporal dimensions, i.e.  $\tau_{i=R}^g = (x^{g,i=R}, t^{g,i=R})$  of the selected UGV  $u_{i=R}^g$ . Lastly, the  $UGVinstances$  is updated with the selected ugv's sortie. Figure 2c shows the recharging UGV's route sortie based on the UAV's rendezvous plan.

Algorithm 1 highlights the overall working principle of  $UGVPlanner$ . The  $UGVPlanner$  is iteratively employed in conjunction with the  $UAVPlanner$ 's strategy for individual UAVs, ensuring efficient coordination between UAVs and UGVs throughout the planning process.

#### B. UAV Planner

The  $UAVPlanner$  constructs the routes of the UAVs asynchronously. Like the  $UGVPlanner$ , the  $UAVPlanner$  also maintains a dictionary  $UAVinstances$  that has structured lists

for all UAVs containing tuples that represent UAVs' coordinate positions at various time points in the global time frame. The UAV whose last timestep value in the time dimension is the least is chosen as the planning UAV  $u_{j=p}^a$  (If multiple UAVs have the same smallest last timestep value, the planning UAV will be chosen arbitrarily among them). Once the planning UAV is chosen, *UAVPlanner* communicates with the *UGVPlanner* to get the available refuel stops  $X^r$  offered by different UGVs and respective time windows  $T^r$  of them. With the available refuel stops and time windows, the *UAVPlanner* models the UAV routing problem as an open-ended energy-constrained vehicle routing problem with time window constraints (O-EVRPTW) with the objective of reducing the age period of the task sites. While planning for UAV  $u_{j=p}^a$  at the planning instance  ${}^Gt_s^{a,j=p}$ , we have to block certain task points that have already been assigned to other UAVs in future time steps. The available task points  $\mathcal{M}_a$  can be defined as:

$$\mathcal{M}_a = \{m_k \in \mathcal{M} \mid m_k \notin \text{UAVinstances}[u_{j \neq p}^a] \text{ for } t \geq t_s^{a,j=p}\} \quad (8)$$

The formulation for O-EVRPTW can be explained with graph theory. Let the available task sites  $\mathcal{M}_a$  and refuel stops  $X^r$  act as the vertices  $V = \mathcal{M}_a \cup X^r$  and  $E = \{(i, j) \mid i, j \in V, i \neq j\}$  denotes the edges connecting vertices  $i$  and  $j$ . We assign non-negative arc cost between vertices  $i$  and  $j$  as  $t_{ij}$  (traversal time) and the decision variable as  $x_{ij}$  that indicates whether a vehicle transits from  $i$  to  $j$ ; also, binary variable  $y_i$  indicates if node  $i$  is visited or not. The UAV commences its journey at starting point  $S$ , visits the task points, and when needed, terminates its route to recharge on a UGV at any available refuel stop  $X^r$ , which are bounded by time-windows due to UGV's slower pace. The objective function, as defined in Eq. 9, is minimizing the cumulative travel duration while dropping the least number of task points. This is achieved by imposing a penalty proportional to the cube of the current *age period* of the dropped mission point,  $P = (a^i)^3$ . This formulation ensures that the UAV prioritizes visiting mission points with a higher age period to avoid incurring significant penalties. Eq. 10 ensures that only one refuel stop is chosen where the UAV ends its route for recharging. We've established energy constraint in Eqs. 11 - 12 to make sure that the UAV never runs out of its fuel and its fuel consumption follows the UAV's power consumption profile during traversal (Eq. 13). The time-window condition in Eq. 14 makes the UAV visit the UGV only after its arrival at any refuel stop  $X^r$ . Eq. 15 says that the cumulative arrival time at  $j^{th}$  node is equal to the sum of the cumulative time at the node  $i$ ,  $t_i$  and the travel time between them  $t_{ij}$ . In both Eq. 13 & Eq. 15 we have applied Miller-Tucker-Zemlin (MTZ) formulation [25] by adding large constant  $L_1, L_2$  for sub-tour elimination in the UAV route. The other generic constraints for a VRP, like flow conservation, are not shown in the paper due to space limits. However, details can be found in our previous works [17], [24].

Objective:

$$\min \sum_i \sum_j t_{ij} x_{ij} + P \sum_i (1 - y_i) \quad \forall i, j \in V \quad (9)$$

Major constraints:

$$\sum_i y_i = 1 \quad \forall i \in X^r \quad (10)$$

$$f_i^a = F^a, \quad i \in X^r \quad (11)$$

$$0 \leq f_i^a \leq F^a, \quad \forall i \in V \setminus \{S, X^r\} \quad (12)$$

$$f_j^a \leq f_i^a - (\mathcal{P}^a t_{ij} x_{ij}) \\ + L_1 (1 - x_{ij}), \quad \forall i, j \in V \setminus \{S, X^r\} \quad (13)$$

$$t_{i,start} \leq t_i \leq t_{i,end}, \quad \forall i \in X^r \quad (14)$$

$$t_j \geq t_i + (t_{ij} x_{ij}) - L_2 (1 - x_{ij}), \quad \forall i, j \in V \quad (15)$$

The UAV route sortie  $\tau_{j=p}^a$  is calculated by the *UAVPlanner* by solving the above O-EVRPTW formulation with Google OR-Tools™ CP-SAT solver [26] that uses constraint programming (CP) and we can utilize different metaheuristics in the solver for avoiding the local optimal solution. The end coordinate and time of the sortie determine the rendezvous time  $t^R$ , rendezvous location  $x^R$ , and the specific UGV,  $u_{i=R}^g$ , chosen for the rendezvous. This information is then fed back to the *UGVPlanner* to complete the UGV sortie as described earlier. The coordinates and temporal components  $\tau_{j=p}^a = (x^{a,j=p}, t^{a,j=p})$  are updated in the *UAVinstances*. After obtaining UGV sortie  $\tau_{i=R}^g$  and UAV sortie  $\tau_{j=p}^a$  from *UGVPlanner* and *UAVPlanner* respectively, we proceed through the *RechargePlanner* to get the recharging path where the UAV travels with the UGV while getting recharged.

### C. Recharge Planner

The *RechargePlanner* calculates the fuel consumption by the UAV  $u_{j=p}^a$  in its sortie and decides how long the UAV  $u_{j=p}^a$  and UGV  $u_{i=R}^g$  should travel together for recharge completion. Based on fuel consumption the recharging time is calculated using Eq. 2, as  $t_{Re}^{a,j=p} = \frac{\mathcal{P}^a \times (t^R - t_s^{a,j=p})}{\beta}$ . During recharging, both vehicles travel together along the UGV's direction  $\vec{X}_{g,i=R}$  as decided in 'direction setting' inside *UGVPlanner* and we get the recharge path  $\tau_{i=R,j=p}^r$ . When the refueling process is completed, the next available point on the road network becomes the take-off place for the UAV  $u_{j=p}^a$  in its next planning instance. As the UGV and UAV travel together their coordinates and times,  $\tau_{i=R,j=p}^r = (x^{r,i=R,j=p}, t^{r,i=R,j=p})$  are added to the *UGVinstances* and *UAVinstances* respectively.

In summary, when the optimization framework plans for UAV  $u_{j=p}^a$ , we get complete sorties for that planning UAV  $u_{j=p}^a$  and its corresponding recharging UGV  $u_{i=R}^g$  through the interactions of *UGVPlanner*, *UAVPlanner*, and *RechargePlanner*. The framework plans asynchronously for all the UAVs, one at a time, until the end of the mission planning horizon is reached. At the end of the mission, we achieve persistent surveillance routes for all UAVs and UGVs throughout the mission period.

#### IV. RESULTS & DISCUSSION

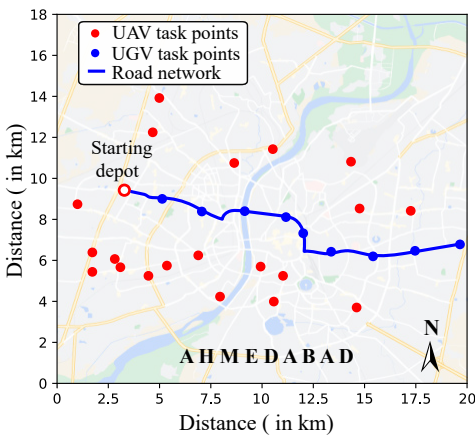


**Fig. 3:** Case study scenario with task sites, road network, and starting depot

The feasibility of our proposed multi-agent collaborative framework, aimed at persistent surveillance for disaster management, is evaluated through a case study simulation centered on the 2001 Gujarat earthquake. This catastrophic event, one of the most severe earthquakes in history, struck the western state of India, resulting in over 20,000 deaths and widespread destruction of infrastructure [27]. Ahmedabad city, situated 225 km from the epicenter, suffered immensely due to its high population density. For our simulation, we have selected a densely populated area within Ahmedabad city to model the disaster management scenario. The simulation's road network, which dictates the paths for the UGVs is accurately mapped based on the city's actual geography. Additionally, we strategically sample a total of 30 task sites following a normal distribution around this road network (see figure 3). Some of these task sites, located directly on the road network, are accessible by both UAVs and UGVs, and sites positioned outside the road network are accessible exclusively to the UAVs, reflecting the operational constraints typical in disaster scenarios. All the simulations are executed within a Python 3.9 environment running on AMD Ryzen 3 5400U processor and 8 GB RAM under a 64-bit operating system.

To align with our study's goals, we have rigorously tested the robustness and scalability of our proposed optimization framework by undertaking a 4-hour persistent surveillance simulation across five different UAV-UGV team configurations: 1 UAV-1 UGV, 2 UAVs-1 UGV, 2 UAVs-2 UGVs, 3 UAVs-2 UGVs, and 4 UAVs-2 UGVs systems. It is assumed that all UAVs and UGVs commence their missions from a fixed starting depot with constant speeds of 10 m/s and 4.5 m/s, respectively, and UAVs have a fuel capacity of 287.7 kJ. During their missions, UAVs are capable of getting recharged from the UGVs, with the limitation of UGVs' capacity constraint. Despite increasing the number of agents, our framework adeptly manages the various team compositions, ensuring successful persistent surveillance by creating conflict-free recharging schedules between UAVs

and UGVs. The effectiveness of our approach is highlighted in the depiction of conflict-free recharging schedules in figure 4 for the 4 UAVs-2 UGVs system where we have the maximum number of vehicles.

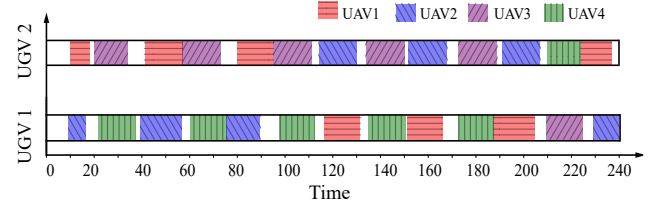


**Fig. 4:** Conflict free recharging schedules of UAVs on UGVs in the 4 UAVs- 2UGVs system

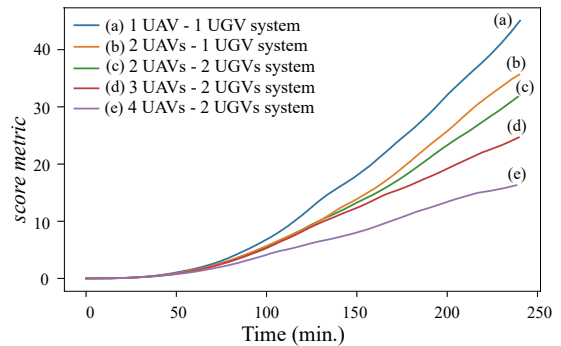


**Fig. 5:** Score metric vs time across different systems

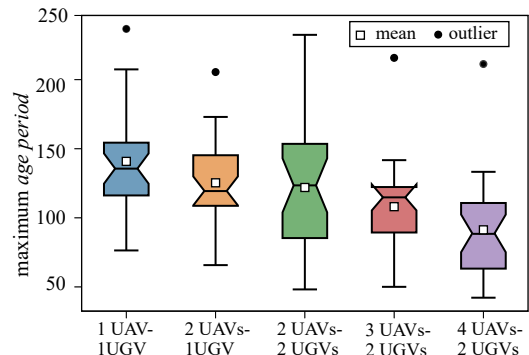


**Fig. 6:** Maximum age period of the task points during persistent surveillance across different systems

Besides planning, we also analyze how different team compositions impact the mission score metric. The figure 5 shows the score metrics of the mission, over the time for the five systems. Notably, the 4 UAVs-2 UGVs system achieves the lowest score metric as desired, whereas the 1 UAV-1 UGV system exhibits the poorest performance. The figure 6 also reveals the distribution of maximum age period across mission points under each system, with the 4 UAVs-2 UGVs setup achieving 35% less mean maximum age period compared to the 1 UAV-1 UGV system. Besides team configuration, the spatial coordinates of task sites significantly influence persistent surveillance outcomes. The figure 7 illustrates the total number of visits to each mission point across different systems at the end of the 4-hour surveillance period. Mission points situated further from the

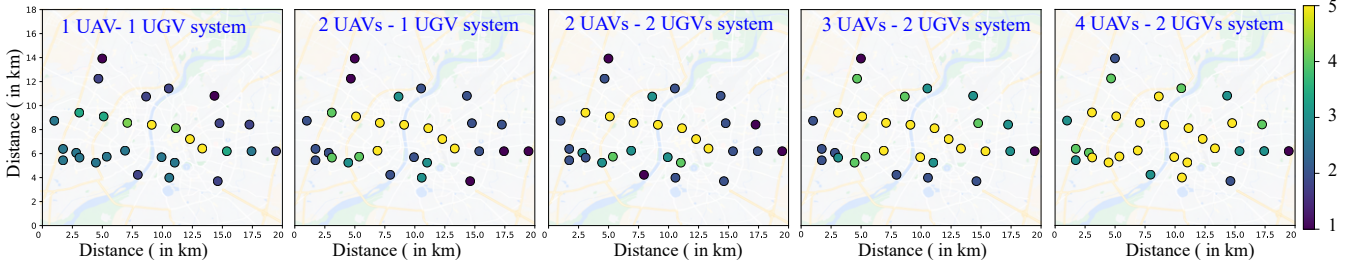


**Fig. 7:** Number of visits to task sites upon mission completion across various systems. The route animations can be found at <http://tiny.cc/x55bvz>

**TABLE I:** Performance analysis of the different systems

System	score metric	Energy cost			CIF
		UAV	UGV	Total	
1 UAV-1 UGV	45.07	1.77	21.19	22.96	0.44
2 UAVs-1 UGV	31.77	3.60	23.37	26.97	0.36
2 UAVs-2 UGVs	31.38	3.55	41.96	45.52	0.60
3 UAVs-2 UGVs	24.67	5.19	47.40	52.59	0.55
4 UAVs-2 UGVs	16.30	7.19	44.15	51.33	0.35

road network experience fewer visits compared to the closer task sites. However, systems equipped with multiple UAVs, thanks to the conflict-free scheduling by the *UAVPlanner*, are able to visit distant points more frequently compared to a single UAV setup. While the 4 UAVs-2 UGVs system demonstrates efficient surveillance capabilities, performance doesn't strictly scale with the number of agents. Systems with 2 UAVs-2 UGVs and 3 UAVs-2 UGVs show performance levels similar to the 2 UAVs-1 UGV system, despite having more number of UGVs. This can be attributed to the UGVs' limitation of recharging only one UAV at a time. Through alternate scheduling between two UAVs one UGV can efficiently perform routing, suggesting that any UAV:UGV ratio below 2:1 introduces a diminishing return on additional UGVs. This is particularly true given UGVs' slower speeds and their restriction to the road network.

This necessitates an efficient cost analysis of the various systems. By following the power consumption profiles (see section II) of the UAVs and UGVs, we have calculated the total energy cost for each system as shown in Table I. It is observed that although systems with a higher number of agents yield lower score metrics, they consume more energy. For ideal persistent surveillance in disaster management, the goal is to achieve the lowest score metric with minimal energy consumption. To facilitate this tradeoff between cost and performance, we conducted a cost analysis by introducing the Cost Inefficiency Factor (CIF), which is defined as follows:

$$\text{CIF} = \frac{S}{S_{max}} \times \frac{C}{C_{max}} \quad (16)$$

here,  $S$  = score metric,  $S_{max}$  = maximum score metric and  $C$  = total cost,  $C_{max}$  = maximum total cost. From the figure 8, the 4 UAVs-2 UGVs system is identified as the most efficient as it has the lowest CIF, and systems with a UAV:UGV ratio less than 2:1 exhibit a higher CIF due to diminishing returns.

Furthermore, we have tested three different metaheuristic methods: Guided Local Search (GLS), Tabu Search (TS), and

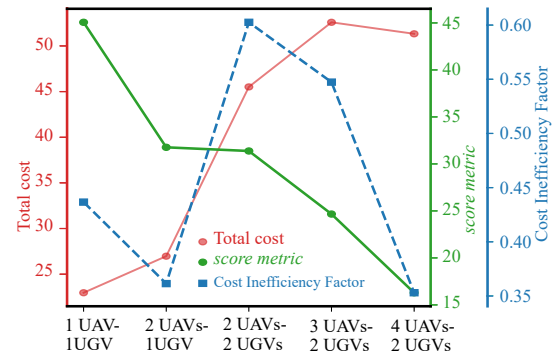


**Fig. 8:** Tradeoff between the performance and cost across the five systems

Simulated Annealing (SA), offered by Google OR-Tools™ CP-SAT solver [26] within the *UAVPlanner*. Table II presents the results of performance metrics for the different team compositions using these metaheuristics. The Tabu Search method consistently outperforms the other methods across most team compositions. Additionally, systems with a greater number of agents show increased solver time consumption, which is attributed to the asynchronous planning architecture of our proposed optimization framework.

## V. CONCLUSION

In this study, we have developed a collaborative routing problem for multiple UAVs and UGVs to enable persistent surveillance in disaster-stricken areas, essential for continuous monitoring and strategic planning in disaster management. By incorporating realistic operational constraints such as UAV fuel limitations, non-instantaneous recharging, UGV speed, and capacity limitations, our approach ensures practical applicability in real-world scenarios. Our proposed framework features dedicated planners for UAVs, UGVs, and the recharging process. It constructs routes for UAVs and UGVs and facilitates conflict-free recharging scheduling between them through high-level asynchronous planning. A case study on a real-world task site with 30 mission points for a 4-hour surveillance operation, across five diverse UAV-UGV teams demonstrates the robustness of our framework. Performance evaluation using a *score metric* reveals that a team with 4 UAVs and 2 UGVs is the most effective, achieving a 63.73% lower *score metric* than a single UAV-UGV team. However, increasing the number of agents does not linearly improve performance due to the

**TABLE II:** Performance comparison of metaheuristics across different systems

Metaheuristics	1 UAV - 1 UGV			2 UAVs - 1 UGV			2 UAVs - 2 UGVs			3 UAVs - 2 UGVs			4 UAVs - 2 UGVs		
	score metric	gap	time	score metric	gap	time	score metric	gap	time	score metric	gap	time	score metric	gap	time
<b>GLS</b>	55.34	22.79	214.91	40.21	26.57	429.63	<b>33.03</b>	<b>0.00</b>	553.99	29.26	18.61	766.59	18.28	12.15	859.05
<b>TS</b>	<b>45.07</b>	<b>0.00</b>	214.40	<b>31.77</b>	<b>0.00</b>	429.69	33.38	1.06	493.16	<b>24.67</b>	<b>0.00</b>	765.54	<b>16.30</b>	<b>0.00</b>	890.35
<b>SA</b>	63.44	40.76	214.15	63.73	100.60	429.73	47.83	44.81	584.57	36.54	48.12	769.67	22.43	37.61	859.11

additional energy costs associated with larger teams. Through meticulous cost analysis, we have further determined that the 2 UAVs-2 UGVs configuration is suboptimal from the cost perspective, and a UAV:UGV ratio below 2:1 leads to diminishing returns due to the high energy expenditure of UGVs. This finding is crucial for identifying the most effective team composition for our persistent surveillance operation. In summary, the framework we propose is not only effective in facilitating complex route planning for multi-agent UAV-UGV teams but also serves as a tool for discerning the optimal team setup based on cost-efficiency metrics. Future research will expand upon this work by incorporating dynamic task point assignment and variable vehicular parameters, enhancing the framework's adaptability to the inherent unpredictability of disaster management. We plan to update task scenarios dynamically at every UAV and UGV rendezvous, allowing mission planners to adjust routes in response to new developments. This approach to stochastic planning merits further investigation as a promising direction for our future work.

## REFERENCES

- [1] Jibin Rajan, Sachin Shrivastav, Abhishek Kashyap, Ashwini Ratnoo, and Debasish Ghose. Disaster management using unmanned aerial vehicles. In *Unmanned Aerial Systems*, pages 129–155. Elsevier, 2021.
- [2] Ged F Griffin. The use of unmanned aerial vehicles for disaster management. *Geomatica*, 68(4):265–281, 2014.
- [3] MZ Naser and VK Kodur. Concepts and applications for integrating unmanned aerial vehicles (uav’s) in disaster management. *I, 5(1):091, 2020.*
- [4] Quanlong Feng, Jiantao Liu, and Jianhua Gong. Urban flood mapping based on unmanned aerial vehicle remote sensing and random forest classifier—a case of yuyao, china. *Water*, 7(4):1437–1455, 2015.
- [5] Arman Nedjati, Bela Vizvari, and Gokhan Izbirak. Post-earthquake response by small uav helicopters. *Natural Hazards*, 80:1669–1688, 2016.
- [6] Robin R Murphy and Sam Stover. Rescue robots for mudslides: A descriptive study of the 2005 la conchita mudslide response. *Journal of Field Robotics*, 25(1-2):3–16, 2008.
- [7] Yu Wu, Shaobo Wu, and Xinting Hu. Cooperative path planning of uavs & ugv for a persistent surveillance task in urban environments. *IEEE Internet of Things Journal*, 8(6):4906–4919, 2020.
- [8] Iván Maza, Fernando Caballero, Jesús Capitán, José Ramiro Martínez-de Dios, and Aníbal Ollero. Experimental results in multi-uav coordination for disaster management and civil security applications. *Journal of intelligent & robotic systems*, 61:563–585, 2011.
- [9] Milan Erdelj, Enrico Natalizio, Kaushik R Chowdhury, and Ian F Akyildiz. Help from the sky: Leveraging uavs for disaster management. *IEEE Pervasive Computing*, 16(1):24–32, 2017.
- [10] N Nikhil, SM Shreyas, G Vyshnavi, and Sudha Yadav. Unmanned aerial vehicles (uav) in disaster management applications. In *2020 Third International Conference on Smart Systems and Inventive Technology (ICSSIT)*, pages 140–148. IEEE, 2020.
- [11] Jürgen Scherer and Bernhard Rinner. Persistent multi-uav surveillance with energy and communication constraints. In *2016 IEEE international conference on automation science and engineering (CASE)*, pages 1225–1230. IEEE, 2016.
- [12] Samira Hayat, Evgen Yanmaz, Timothy X Brown, and Christian Bettstetter. Multi-objective uav path planning for search and rescue. In *2017 IEEE international conference on robotics and automation (ICRA)*, pages 5569–5574. IEEE, 2017.
- [13] Wei Gao, Junren Luo, Wanpeng Zhang, Weilin Yuan, and Zhiyong Liao. Commanding cooperative ugv-uav with nested vehicle routing for emergency resource delivery. *IEEE Access*, 8:215691–215704, 2020.
- [14] Subramanian Ramasamy, Md Safwan Mondal, Jean-Paul F Reddinger, James M Dotterweich, James D Humann, Marshal A Childers, and Pranav A Bhounsule. Heterogenous vehicle routing: comparing parameter tuning using genetic algorithm and bayesian optimization. In *2022 International Conference on Unmanned Aircraft Systems (ICUAS)*, pages 104–113. IEEE, 2022.
- [15] Subramanian Ramasamy, Md Safwan Mondal, Jean-Paul F Reddinger, James M Dotterweich, James D Humann, Marshal A Childers, and Pranav A Bhounsule. Solving vehicle routing problem for unmanned heterogeneous vehicle systems using asynchronous multi-agent architecture (a-teams). In *2023 International Conference on Unmanned Aircraft Systems (ICUAS)*, pages 95–102. IEEE, 2023.
- [16] Kevin Leahy, Dingjiang Zhou, Cristian-Ioan Vasile, Konstantinos Oikonomopoulos, Mac Schwager, and Calin Belta. Persistent surveillance for unmanned aerial vehicles subject to charging and temporal logic constraints. *Autonomous Robots*, 40:1363–1378, 2016.
- [17] Md Safwan Mondal, Subramanian Ramasamy, James D Humann, Jean-Paul F Reddinger, James M Dotterweich, Marshal A Childers, and Pranav A Bhounsule. Cooperative multi-agent planning framework for fuel constrained uav-ugv routing problem. *arXiv preprint arXiv:2309.03397*, 2023.
- [18] Kenny Chour, Jean-Paul Reddinger, James Dotterweich, Marshal Childers, James Humann, Sivakumar Rathinam, and Swaroop Darbha. A reactive energy-aware rendezvous planning approach for multi-vehicle teams. In *2022 IEEE 18th International Conference on Automation Science and Engineering (CASE)*, pages 537–542. IEEE, 2022.
- [19] Sepehr Seyedi, Yasin Yazıcıoğlu, and Derya Aksaray. Persistent surveillance with energy-constrained uavs and mobile charging stations. *IFAC-PapersOnLine*, 52(20):193–198, 2019.
- [20] Xiaoshan Lin, Yasin Yazıcıoğlu, and Derya Aksaray. Robust planning for persistent surveillance with energy-constrained uavs and mobile charging stations. *IEEE Robotics and Automation Letters*, 7(2):4157–4164, 2022.
- [21] Arnon M Hurwitz, James M Dotterweich, and Trevor A Rocks. Mobile robot battery life estimation: battery energy use of an unmanned ground vehicle. In *Energy Harvesting and Storage: Materials, Devices, and Applications XI*, volume 11722, pages 24–40. SPIE, 2021.
- [22] Nabil H Mustafa and Saurabh Ray. Improved results on geometric hitting set problems. *Discrete & Computational Geometry*, 44:883–895, 2010.
- [23] Parikshit Maini and PB Sujit. On cooperation between a fuel constrained uav and a refueling ugv for large scale mapping applications. In *2015 international conference on unmanned aircraft systems (ICUAS)*, pages 1370–1377. IEEE, 2015.
- [24] Md Safwan Mondal, Subramanian Ramasamy, James D Humann, Jean-Paul F Reddinger, James M Dotterweich, Marshal A Childers, and Pranav Bhounsule. Optimizing fuel-constrained uav-ugv routes for large scale coverage: Bilevel planning in heterogeneous multi-agent systems. In *2023 International Symposium on Multi-Robot and Multi-Agent Systems (MRS)*, pages 114–120. IEEE, 2023.
- [25] Clair E Miller, Albert W Tucker, and Richard A Zemlin. Integer programming formulation of traveling salesman problems. *Journal of the ACM (JACM)*, 7(4):326–329, 1960.
- [26] Google. Google OR-tools. <https://developers.google.com/optimization>, 2021. Online; accessed Feb 2, 2021.
- [27] M Yanger Walling and William K Mohanty. An overview on the seismic zonation and microzonation studies in india. *Earth-Science Reviews*, 96(1-2):67–91, 2009.